Journal of Biological Physics
https://doi.org/10.1007/s10867-019-09528-2

ORIGINAL PAPER

Ellipsometric-based novel DNA biosensor for label-free, real-time detection of *Bordetella parapertussis*

S. Rafique[1] · M. Idrees[2] · H. Bokhari[2] · A. S. Bhatti[3]

Received: 27 July 2018 / Accepted: 24 June 2019/Published online: 02 August 2019

Abstract

Pertussis (or whooping cough) is a contagious disease mainly affecting infants and children and predominantly caused by *Bordetella pertussis* followed by *Bordetella parapertussis*. *B. parapertussis* causes a milder cough but usually symptomatically appears like *B. pertussis* infection. Thus the epidemiology of illness caused by *B. parapertussis* is not well understood. In this study, a sensitive and specific method for the rapid diagnosis of *B. parapertussis* is presented. The covalent immobilization of thiol-terminated DNA oligonucleotides (ss DNA SAM) on a silicon surface by disulfide bond formation is investigated with atomic force microscopy (AFM) and ellipsometry. The measurements indicated an average layer thickness of 5 ± 0.84 nm for 2 μg/μl concentration and 24 h incubation time. This thickness changed to 8.4 ± 0.92 nm for the same concentration (2 μg/μl) by altering the incubation time to 48 h. Ellipsometric data recorded before and after hybridization of *B. parapertussis* revealed an increase in mean grain area from 91 nm^2 to 227 nm^2 and a change in the refractive index from 1.489 to 1.648 for 2 μg/μl *B. parapertussis*, respectively. This change in the refractive index was used to evaluate the amount of adsorbed molecules and their density. The results showed that the density of adsorbed molecules increased from 0.2 to 0.97 g/cm^3 after *B. parapertussis* attachment, respectively. To confirm the hybridization of *B. parapertussis* to ss DNA SAM, the ds DNA SAM was denatured and the ss DNA SAM surface was reproduced with an average height variation of 6.42 ± 0.75 nm. This showed the stability of the DNA film that can be tuned by varying the concentration and incubation time, thus providing a robust method for the label-free detection of *B. parapertussis* other than routinely used PCR detection.

Keywords Whooping cough · *Bordetella parapertussis* · Self-assembled monolayer · Ellipsometry · DNA · Hybridization

✉ S. Rafique
saima.rafique@mail.au.edu.pk

Extended author information available on the last page of the article

1 Introduction

Bordetella pertussis is the major causative agent of the respiratory disease pertussis (whooping cough), followed by *Bordetella parapertussis,* which is most severe for infants. It is a current health problem that occurs worldwide with a high prevalence among young unvaccinated infants [1] and it is a major cause of death in children. The impact of *B. parapertussis* as a causative agent of whooping cough is underestimated. This is mainly due to the fact that *B. parapertussis* infection is usually misdiagnosed as *B. pertussis* due to similar symptoms [2]. This is further complicated when current vaccines are targeting *Bordetella pertussis* as the sole causative agent of whooping cough where *B. parapertussis* is circulating predominantly [3]. Therefore the wide prevalence of parapertussis and its changing epidemiology have highlighted the need for rapid and sensitive methods (such as biosensors) for diagnosing *B. parapertussis*.

To date, few studies have been conducted on the management of parapertussis [4]. As many persons infected with *B. parapertussis* are asymptomatic and the majority have a mild course, many infections remain undetected. These persons can act as carriers of infection and may transmit the disease to young infants, who may have a severe course. In fact, fatality from parapertussis has been reported [5]. Thus, early diagnosis and treatment can help to develop better preventive and control strategies.

Laboratory methods for the diagnosis of parapertussis are traditionally based on culture or a positive PCR assay [6, 7]. The culturing depends on specimen quality, rapid transportation, and laboratory expertise. The culture method may take 3 to 7 days. It lacks in sensitivity but is highly specific for *B. parapertussis* detection in comparison to PCR [8, 9]. For example, Lena et al. (1998) diagnosed *B. pertussis* and *B. parapertussis* infections by PCR and culture methods. The results obtained by both methods were compared and showed that the overall sensitivity by PCR was 65%, which was higher than that of culture 58% [10]. Similarly, Valentina et al. (2014) developed real-time multiplex PCR that uses target IS481, IS1001, and human GAPDH gene for detection of *B. parapertussis*. They compared an assay of *B. parapertussis* infection with clinical standards and showed that sensitivity was 5, 59, and 89% and the specificity was 100, 100, and 100% for culture, conventional, and multiplex real-time PCR, respectively [11]. Therefore, compared to culture, PCR is one of the most effective tools being used as a diagnostic test for detection and differentiation of *B. pertussis* and *B. parapertussis* DNA [12].

Due to the contagiousness of parapertussis, a rapid and sensitive method for diagnosis is required to initiate the treatment and interrupt its transmission. DNA biosensors have been used as a rapid tool for cost-effective detection of pathogens but they lack sensitivity [13, 14]. The driving force behind DNA biosensor development lies in the tremendous potential for obtaining sequence specific information in a faster, cheaper, and more reliable manner as compared to traditional hybridization assays [15].

Various studies have reported the sensitive and label-free biosensing of RNA and DNA by studying the nature of interaction between probe and target. Touahir et al. (2010) studied the various reactions paths and conditions allowing anchoring of a DNA oligomer to a silicon surface (substrate) [16]. Georgiadis et al. (2000) studied the quantitative measurements and modeling of kinetics in nucleic acid using SPR spectroscopy. They showed that the presence of thiol functionality on a 25-mer ss DNA (single stranded DNA) give rise to adsorption behavior that is clearly kinetically distinct from simple ss DNA adsorption on gold [17]. Similarly, Li et al. (2017) reported fast and sensitive

immunosensing of immunoglobulin G (IgG) using an ellipsometer. They observed a difference in the refractive index with respect to a change in Δ (phase difference). They observed a Δ change of 0 to 20° and a refractive index change of 1.33 to 1.34 with a variation of angle of incidence from 67 to 75° [18]. For performance of the biosensor, the experimental results showed that the limit of detection for IgG was 15 ng/ml and the data collection time was in milliseconds.

Information concerning the immobilization of single-stranded DNA (ss DNA) and double-stranded DNA (ds DNA) on a surface is paramount to the development of a DNA based optical biosensor. At present, PCR and culture methods are employed in Pakistan for diagnosis of *B. parapertussis* [19]. In this current study, we employ a novel biosensing approach (optical technique) for label-free detection of a nucleic acid sequence (by developing a self-assembled monolayer on a gold surface) for detecting a commonly circulating whooping cough pathogen in Pakistan.

2 Methods

2.1 Buffers

The two types of buffer were prepared in double-distilled water and used for the immobilization and washing of DNA-SAM (self-assembled monolayer) on a biosensor substrate after every step of preparation

Buffer 1 100 mM Tris (Sigma Aldrich) and 100 mM sodium chlorate (Sigma Aldrich) with pH = 7.5.
Buffer 2 50 mM Tris (Sigma Aldrich) and 50 mM sodium chlorate with pH = 8.6

2.2 DNA sequence

The modified (Thiol labeled) DNA sequence targeting the *B. parapertussis* specific DNA sequence (IS1002) was commercially synthesized with the following base sequence:

1. SS-5′-TTCAGGCACACAAACTTGATGGGCG-3′
2. 5′-CGCCCATCAAGTTTGTGTGCCTGAA-3′ (Complementary of 1)

where SS-5′ refers to HO_3PO-$(CH_2)_6$-SS-$(CH_2)_6$-OH. The *B. parapertussis* clinical isolate from our previous study (Bokhari et al. 2011) was used as the target DNA sequence [3].

2.3 Preparation of DNA SAM biosensor

2.3.1 Substrate preparation

The substrate used in this study was silicon (100) with a size of 5 × 5 mm^2. The substrate was scoured ultrasonically with ethanol and distilled water for 15 min. The 40 nm Au layer was deposited on a silicon substrate in a vacuum chamber at a pressure of 2 ×

10^{-6} Torr. All the instruments were autoclaved before each step of preparation of the DNA SAM biosensor.

2.3.2 Biosensor preparation

The double-stranded DNA (ds DNA) was prepared by hybridization of sequence 1 (5′ thiol-labeled primer sequence) and 2 in buffer 1 for 1 day at DNA concentrations of 2, 5, and 10 μg/μl. The schematic representation of the biosensor is shown in Fig. 1. The Au surface was incubated in the hybridized buffer for different incubation times at room temperature in step 1. After complete formation of the monolayer the surface was rigorously washed with buffer 2. The ss DNA SAM of sequence 1 were attained by dehybridization of ds DNA SAM in a water/ethanol solution for 5 min at 37 °C in step 2. This method produces a more reproducible surface compared to the straight incubation of the Au surface in sequence 1 [20]. In addition, it also limits the exposed base pairs of nitrogen of ss DNA SAM with the Au surface [21]. After dehybridization, the substrate containing ss DNA SAM was removed from the solution, rinsed rigorously with buffer 2 (Tris chlorate, pH = 8.6) for 5 min, and then again incubated in the DNA + Buffer 1 solution. After the organization of ss DNA SAM, the chip was again washed with buffer 2 to remove any unbounded ss DNA SAM. Then the chip was dried by argon. The measurements were performed after 1 day and 2 days of incubation time.

A whole genomic DNA of *B. parapertussis* was used as a target DNA, which was obtained as described by Bokhari et al. [22]. The attachment of target DNA on the ss DNA SAM chip was performed by denaturing the target double strand (ds) in buffer 1. It

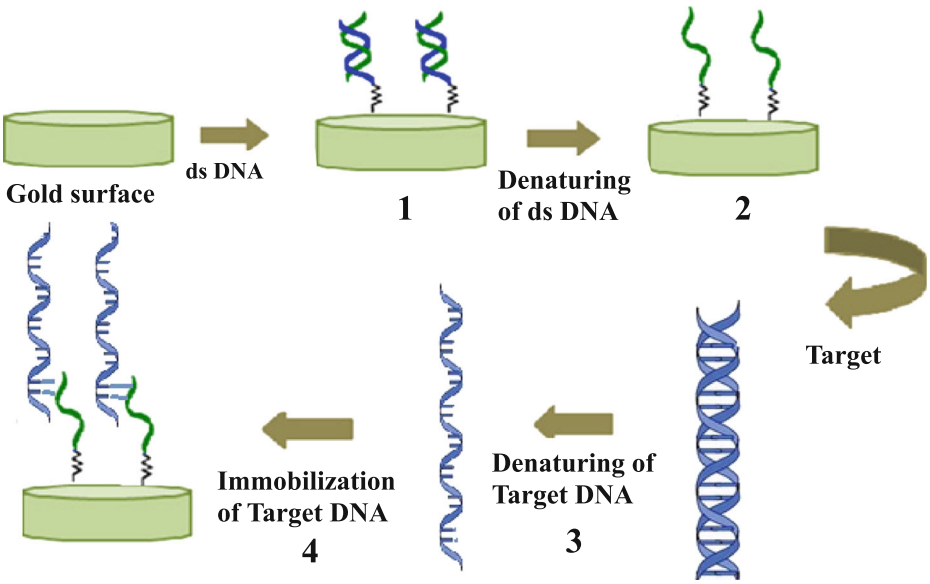

Fig. 1 Schematic representation of the steps followed for the preparation of the *B. Parapertussis* biosensor. The ds DNA SAM were immobilized on the surface in step 1 and then denatured to ss DNA SAM in step 2. In step 3, target DNA was denatured and finally immobilized on ss DNA SAM surface in step 4

was denatured at 95 °C for 5 min and subsequent sharp cooling in step 3. The solution of ss target DNA was used as soon as possible to minimize any potential interactions or cross linking in the solution. The ss DNA SAM immobilized chip was dipped in the denatured ds target DNA solution at 55 °C for a few minutes. The chip was incubated in buffer 1 containing ds target DNA solution for 1 day at room temperature. In this way the ss DNA SAM probe was hybridized with its complementary target DNA in step 4 (Fig. 1). Each sample was rinsed with the excess volume of buffer 2 and dried with a stream of argon before characterization. Similarly, for the control experiment the same process was followed with some random DNA other than the *B. parapertussis* but of same length.

2.4 Characterization

2.4.1 AFM measurements

The surface morphology of the DNA SAM biosensor was studied using Agilent's PicoPlus AFM in tapping mode. The percentage surface coverage was evaluated from tens of AFM images having different sizes. Gwyddion software was used to find the ratio percentage of surface covered with ss DNA SAM to the size of the image. The thickness of the biolayer was obtained by measuring the height variation between the silicon substrate and after attachment of DNA SAM on the substrate. The data were extracted from a large set of measurements for each experiment; data from 20 different 5×5 μm^2 areas were typically combined to generate the data. To quantify the variation in thickness, the root mean square was determined from $RMS = \sqrt{\frac{\sum(Z_i - Z_{avg})^2}{N}}$ in which Z_i = surface elevation, Z_{avg} = mean value of Z_i and N is the number of samples.

2.4.2 Ellipsometric measurement

Ellipsometry was employed to study the adsorption and hybridization of DNA molecules. The vertical structures of the sample, the 'optical' thickness of the layer, were measured using a Sentech Spectroscopic Ellipsometer 850. All the measurements were carried out in air in a wavelength range of 300 to 500 nm at a 70° light reflection angle. In addition, the kinetic measurements of ss DNA SAM and hybridization of DNA molecules were carried out by measuring the $\Psi(\lambda)$ and $\Delta(\lambda)$ spectra for different incubation times as well as for a certain time interval (0–120 min), in which Ψ is the amplitude ratio of incident and reflected light $\tan(\Psi) = {}^{A_p}/_{A_s}$ and Δ is the phase shift $\Delta = \varnothing_p - \varnothing_s$ between the p and s components of the polarized light. The optical parameters, such as thickness (d) and refractive index (n), were obtained by fitting experimental data to the model system using software Spectra Ray/4. The measurement of Δ is preferable as it is ten times more sensitive to the changes in the developed layer parameter than Ψ [23]. The shift in Δ spectra is usually larger compared to Ψ, which makes Δ a good candidate for kinetic study of different chemical and biochemical reactions on the surface. It is also noted that high sensitivity can be achieved for a kinetic study performed by measuring Δ at a fixed wavelength [24]. So, the DNA hybridization kinetic curves were obtained at a particular wavelength (λ) from a large number of Δ files and their time dependencies were plotted with the relative change in $\Delta(t)$.

3 Results and discussion

3.1 Gel electrophoresis

Gel electrophoresis is a standard method used to separate, identify, and analyze the size of DNA fragments. The shift in agarose gel primarily depends on the size of the DNA fragment and the voltage of electrophoresis [25]. Gel electrophoresis (Powerpac basic power supply, Bio-Rad) was conducted under 100 V for 1 h by using 1% agarose gel (Ultrappure) and a 100 bp DNA marker (M) (Fig. 2). Agarose gel electrophoresis showed the successful amplification of a 293-bp DNA segment (Fig. 2; Lanes c, d) of *B. parapertussis*-specific DNA sequence (IS1002) while using the thiol-labeled primer (Fig. 2; Lanes a, b). The PCR-amplified thiol-labeled 293-bp sequence was immobilized in the next steps on a gold chip.

3.2 Height of ss DNA on silicon surface

The immobilization of oligonucleotide on a solid surface is a crucial step for DNA biosensor application. In this study, the ss DNA SAM was immobilized on gold through the thiol. Firstly, the effect of incubation time on ss DNA SAM immobilization (after step 2 in biosensor preparation) was evaluated. For this purpose, the effect of incubation time on different concentrations of ss DNA SAM was investigated. The ss DNA SAM concentrations used were 2, 5, and 10 μg/μl and incubation time varied from 1 to 21 h. The DNA SAM layer thickness was measured through the ellipsometer and all incubations were carried out at room temperature (pH = 7.4). Figure 3a shows the thickness of the ss DNA SAM layer as a function of incubation time for three different concentrations. The thickness of the ss DNA SAM layer on the silicon surface was 1.77, 2.40, and 3.11 nm for 2, 5, and 10 μg/μl during the first hour of incubation. This thickness increased to 6.79, 13.22, and 19.81 nm for 2, 5, and 10 μg/μl in approximately 15 h of incubation and then did not change significantly.

Initially, the thickness increase suggested that the molecules adsorb and form more closely packed morphology and some adsorb randomly on the surface. When the incubation time increased these randomly adsorbed molecules became agglomerated, which increased the thickness of the ss DNA SAM. With a further increase in incubation time, the agglomeration in the solution as well as the surface increased, which further increased the thickness of the

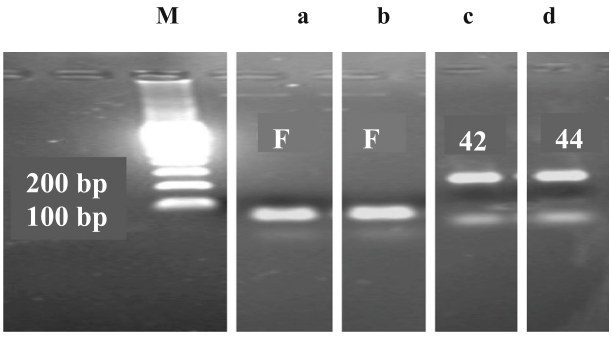

Fig. 2 Agarose gel electrophoresis images of DNA fragments. *Lanes a–b* photo image of agarose gel for small DNA fragments; *Lanes c–d* photo image of agarose gel for target DNA from host species

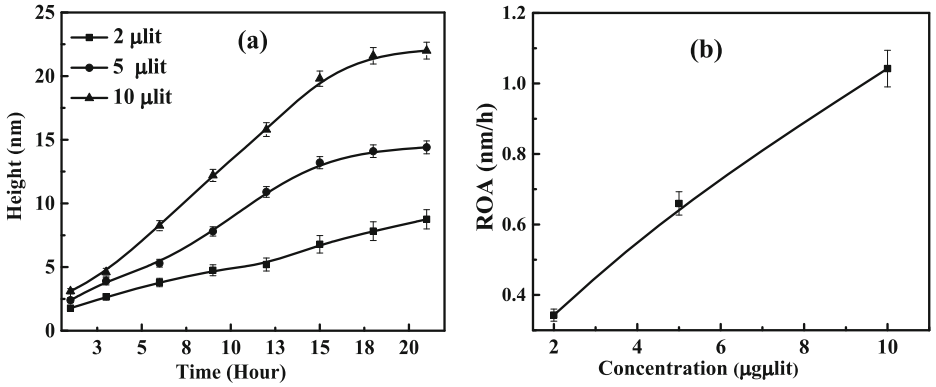

Fig. 3 Ellipsometric measurement of **a** thickness with different concentrations of ss DNA SAM (2, 5, and 10 μg/μl); incubation time varied from 1 to 20 h. **b** Rate of molecule adsorption (ROA) as a function of concentration

layer and after a certain time this agglomeration achieved the saturation value. To investigate this phenomenon, the rate of adsorption, obtained from fitting the curve, for the molecules was evaluated and plotted in Fig. 3b. The rates of molecule adsorption (ROA) were 0.3429 ± 0.0171, 0.6597 ± 0.03295, and 1.0422 ± 0.0521 nm/h for 2, 5, and 10 μg/μl ss DNA SAM concentrations. It is important to note that the thickness of the ss DNA SAM layer on the silicon substrate did not change significantly for 5 and 10 μg/μl after 15 h of incubation. It is of significance that the thickness and rate of adsorption were elevated at a high concentration and reached their saturation value quicker than for a low concentration. It is suggested that more agglomerated molecules adsorb at a high rate for 10 μg/μl ss DNA SAM concentration than at 2 μg/μl ss DNA SAM concentration. So, from here a 2 μg/μl concentration was selected to investigate the hybridization effect on the surface.

3.3 Ellipsometric determination of adsorption of DNA to gold surface

Ellipsometry allows for a direct label-free proof of ss DNA SAM immobilization on the substrate. The main objective of ellipsometry data analysis is to achieve an accurate description of the substrate using the simplest possible model. In the analysis of a modified gold surface, a four-layer structure was built consisting of a substrate/SiO_2/gold/overlayer as shown in Fig. 4a. In the present study, a Cauchy model is used to determine the effective complex index of a layer. The Cauchy dispersion function $n = A + {}^{B}/_{\lambda^2}$ was used to find the different parameters of the ss DNA SAM layer [26], where A and B are the Cauchy parameters. The Cauchy parameters and parameters of the four-layer model were obtained by fitting the obtained ellipsometric spectra, which are given in Table 1. The value of n was obtained at λ = 500 nm; however, the fitting was performed over the whole spectral range. The thickness and refractive index of the layer are impossible to evaluate simultaneously [27], so the thickness obtained from the AFM was used to determine the refractive index of the ss DNA SAM layer.

The reliability of the ellipsometer to differentiate the DNA layer with respect to a bare substrate has been proved with Ψ, or more precisely in reverse order with the Δ angle shown in Fig. 4b, c. The ellipsometric angles Ψ and Δ were dependent on small changes occurring on the substrate. Tikhonravov et al. (1999) evaluated the optical constant for fluoride films by

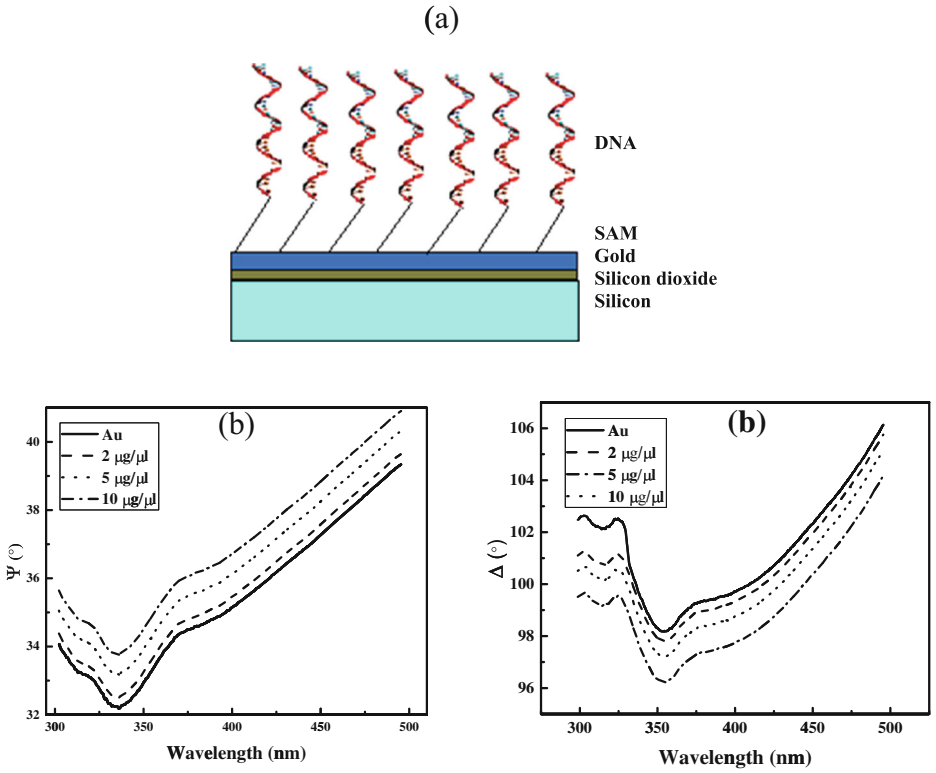

Fig. 4 **a** Description of ellipsometric model used to fit the optical index of ss DNA SAM. **b** Ellipsometry spectra of the angles Ψ and **c** Δ for 2, 5, and 10 μg/μl DNA strands grafted on gold for 1-day incubation time

ellipsometry. They showed that the ellipsometric angle Δ is more sensitive to surface inhomogeneities than the angle Ψ [28]. Similarly, Nabok et al. (2011) showed that both modeling and experiments are more sensitive to Δ for small changes in the thickness and refractive index of the adsorbed layer [29]. The sensitivity primarily comes from the change in delta as shown in Fig. 4b. A small but significant change in Ψ was observed. However, for Δ the curves were more marked for the wavelength lower than 400 nm and the first peak was observed at 102.6, 101.2, 100.7, and 99.7 for Au, 2, 5, and 10 μg/μl, at 302 nm wavelength, respectively. After attachment of ss DNA SAM, the original Δ spectra shifted downward from gold. Fitting with the ellipsometric model provides a thickness of the ss DNA SAM layer of about 5.25 ± 0.95 nm and showed successful attachment to the gold surface. However, the phase shift (Δ) is highly related to the optical properties of the layer from which the light is reflected. A complex index of refraction (i.e., layers deposited on silicon) can easily be associated with layer thickness.

Table 1 Parameters obtained from ellipsometric fitting for 2 μg μl^{-1} and 1-day incubation time. The parameters marked with * were fixed during fitting

SiO_2	n* = 1.457
Au	n* = 0.759 ± 0.088
	d* = 38.8 ± 2.6 nm
Cauchy layer	
A* = 1.407	n* = 1.478
B* = 0.04	

Table 2 Results of ss DNA SAM biosensor thickness, refractive index, adsorbed molecule, and their density for 1-day incubation time grafted on gold surface measured by AFM and ellipsometry

Concentration (μg μl^{-1})	Thickness t (nm)	Refractive index (n)	Amount of adsorbed molecules M (mg/cm^3)	Density of molecules D (g/cm^3)
2	5.23	1.489	1.05	0.2
5	10.16	1.569	5.15	0.62
10	14.40	1.652	15.7	1.08
Target DNA	32.70	1.634	21.3	0.97

Determination of the thickness (d) and refractive index (n) was carried out by the fitting of Ψ and Δ. By fitting, the refractive index (n) was obtained as shown in Table 2. It shows that the thickness was 5.25 ± 0.84, 8.24 ± 0.92, and 14.40 ± 1.22 nm and their refractive index was 1.489, 1.569, and 1.652 for 2, 5, and 10 μg/μl, respectively, for 1-day incubation. Similarly, the thickness changed to 8.41 ± 0.90, 17.56 ± 1.11, and 20.99 ± 1.43 nm and the refractive index changed to 1.594, 1.645, 1.788 for 2, 5, 10 μg/μl, respectively, for 2-day incubation. This increase in thickness was due to the increase in pile size with incubation time. As the incubation time increased, the refractive index increased due to an increase in ss DNA SAM density in ss DNA SAM piles. It was not a simple monolayer of ss DNA SAM for 2 days of incubation time; there were bundles of ss DNA SAM immobilized on the Au surface as can be clearly seen in AFM images.

3.4 AFM analysis of ss DNA SAM immobilization

In order to investigate the film quality and layer structure of the ss DNA SAM surface, atomic force microscopy (AFM) was performed. AFM was used to confirm the thickness obtained from the ellipsometer and the phenomenon occurring for organization of the ss DNA SAM layer before and after saturation as shown in Fig. 5a–g. The bare gold surface is quite homogenous (Fig. 5a) with a surface variation of 2.20 ± 0.43 nm. Modification of ss DNA SAM on the surface with different concentrations and incubation time causes changes on the surface morphology. As seen in Fig. 5b, a smooth and ordered ss DNA SAM layer was observed with a thickness of about 5.25 ± 0.84 nm for 2 μg/μl. It can be seen that as the concentration of ss DNA SAM increased from 2 to 10 μg/μl, the thickness of ss DNA SAM increased from 5.25 ± 0.84 to 14.40 ± 1.22 nm for 1-day incubation time. This suggested that, at a lower concentration (2 μg/μl) a well-covered ss DNA SAM attachment can be observed. With an increase in concentration (5 μg/μl) molecules formed an island-like formation on the Au surface. With a further increase in concentration (10 μg/μl), a larger island was formed with many bundles separated by gaps [30], as can be seen in Fig. 5d. This suggested that as the concentration increased, the thickness and island formation also increased. A similar behavior was observed in the case of 2 days time of incubation. As the incubation time increased, the thickness as well as the island structures formation increased. This showed that the incubation time and concentration both affect the surface morphology of ss DNA SAM. To further understand the ss DNA SAM adsorb layer, the surface coverage was evaluated from different AFM images by using Gwyddion software. Different-sized AFM images were analyzed (by taking the ratio percentage of surface covered with ss DNA SAM to the size of image) to determine the percentage surface coverage. The obtained surface coverage was plotted as a

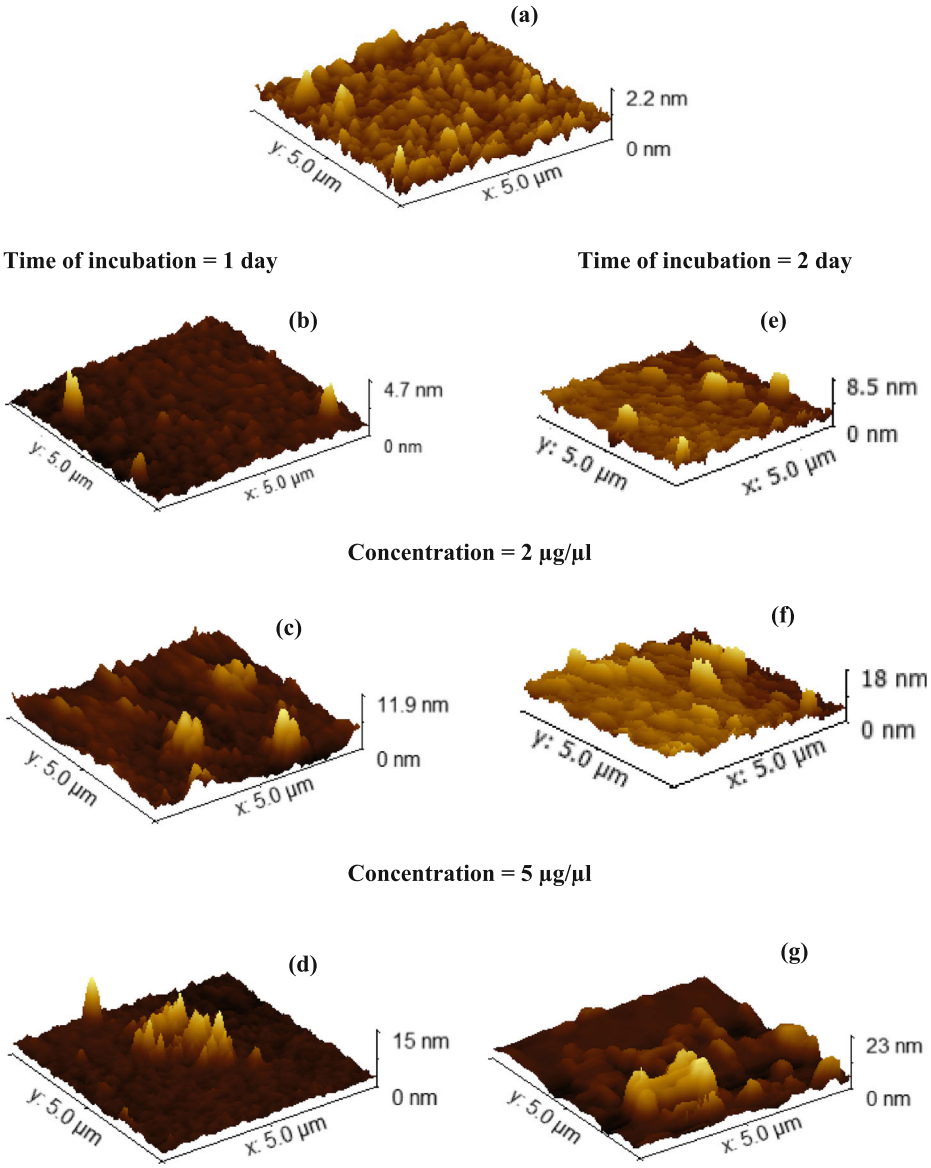

Fig. 5 3D AFM images (5 × 5 µm) of **a** bare gold surface with different concentrations of ss DNA SAM; (1) 2 µg/µl, (2) 5 µg/µl, (3) 10 µg/µl for 1 day (**b**–**d**) and 2 days (**e**–**g**). Incubation times (*darker*: lower amplitudes) and ss DNA SAM (*brighter*: higher amplitudes)

function of concentration, as shown in Fig. 6. It shows that the surface coverage decreased from 70 to 20% as the thickness increased from 5.25 to 14.40 nm for 1-day incubation time. The thickness of ss DNA SAM formed after 1-day incubation time was 5.25 ± 0.84 nm for 2 µg/µl, which is almost a maximum coverage of ss DNA SAM layer with a surface coverage of 70%. However, there was an increase in the thickness to 14.40 ± 1.22 nm for 10 µg/µl (1-day incubation time) and a decrease in surface coverage to 20%. It showed that the ss DNA

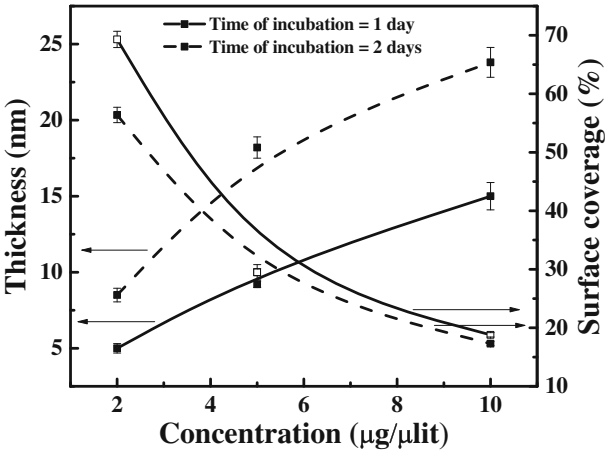

Fig. 6 Thickness and surface coverage evaluated from AFM images for 1 day (*solid line*) and 2 days (*dashed line*) time of incubation

SAM adsorbs on the gold surface as well as interacts with another [31]. This increase in thickness was due to the formation of aggregates at a higher concentration as well as incubation time. These aggregates were due to the fact that ss DNA SAM is highly reactive to form ds DNA due to the presence of small Van der Waals forces between the DNA molecules, which led them to stack one above the other with random orientation. This stacking increased the aggregate size and the appearance of a circular structure at a higher concentration and the incubation time in AFM images was most probably due to the ss DNA SAM aggregation that increased the thickness of the adsorbed ss DNA SAM layer and decreased its surface coverage. Similar effects were observed in the case of 2-day incubation time.

In conclusion, at a high concentration (10 μg/μl), the rate of molecules adsorption was elevated, which resulted in a high value of surface coverage. In the present case, the surface coverage dropped to a lower value (from 70 to 20%) at a high concentration. This suggests that ss DNA SAM molecules were adsorbed on each other, which increased the thickness and saturated the surface coverage earlier compared to a low concentration (2 μg/μl). This implies that, for uniform biosensor surface preparation, the biomolecule solution (ss DNA SAM) concentration and adsorption conditions on the silicon surface are very important.

3.5 Calculation of adsorbed surface density

For ss DNA SAM, adsorption kinetics was studied with ellipsometry with variations in concentrations of ss DNA SAM. The thickness and refractive index were determined by AFM and ellipsometry and the change in the refractive index of ss DNA SAM with increasing concentration was calculated with the De Feitjer formula (Corsel et al. 1986) to determine the amount of bound ss DNA SAM from their thickness [32].

$$M = \frac{d\,(n_A - n_C)}{dn/dC}$$

where M (mg/m^2) is the surface concentration, i.e., the adsorbed surface mass density, d (nm) is the thickness of ss DNA SAM, n_A and n_C are the refractive indices of the ss DNA layer and

buffer and dn/dC (cm^3/g) are the refractive index increments. The density of the film D = M/d (g/cm^3) was calculated and the values obtained for 1-day incubation are shown in Table 2. It can be seen that the adsorbed mass of ss DNA SAM and their density increased with an increase in concentration. A general profile obtained for the growth of ss DNA SAM film is shown in Fig. 7. The assembly of the film is characterized by an increase in both the thickness and the mass of the film as well as an increase in the density of the film. With the elevation in concentration, the amount of adsorbed molecules increased from 1.05 to 5.5 mg/cm^3. With a further elevation in concentration to 10 μlit, the amount of adsorbed molecules increased to 15.7 mg/cm^3. It shows that the number of adsorbed molecules increased and an assemblage of aggregates on the surface as can be seen in the AFM image. Interestingly, the surface coverage decreased with an increase in concentration. It is highly probable that with increase in concentration and incubation time the oligonucleotides agglomerate in the solution that assembled as an aggregate on the surface of gold. This in turn increased the molecule adsorption and density but decreased the surface coverage [33].

3.6 Hybridization on a modified surface

Hybridization of ss DNA SAM with its target DNA from host species was performed on 2 μg/μl ss DNA SAM. This concentration was selected as the experimental thickness of ss DNA SAM film as it matches with the theoretical value reported by Yun et al. [34] and the highest surface coverage was obtained for this concentration. An immobilization of *B. Parapertussis* obtained from host species causes a change on the surface morphology as well as on the optical spectra obtained from an ellipsometer.

In order to monitor the hybridization process, different concentrations of target DNA ranging from 0.1 to 2 μg/μl were used. The film quality and layer structure of the prepared surface was investigated by AFM. Figure 8a–g gives the AFM images of the surface. The first image (a) is for the ss SAM DNA, 2 μg/μl concentration. The surface is quite homogenous (Fig. 8a) with a thickness of 5.25 ± 0.84 nm, while with the immobilization of target DNA the surface morphology changed. The adsorption of non-complementary DNA (control) on the adsorbed DNA resulted in much smaller changes in the thickness (6.2 ± 0.89 nm)

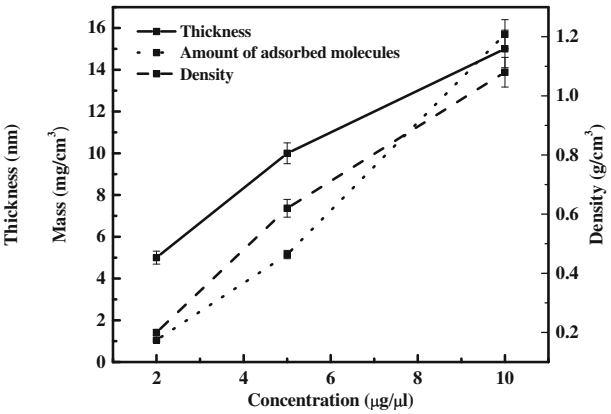

Fig. 7 The density and amount of adsorbed ss DNA SAM on gold surface as a function of ss DNA SAM concentration

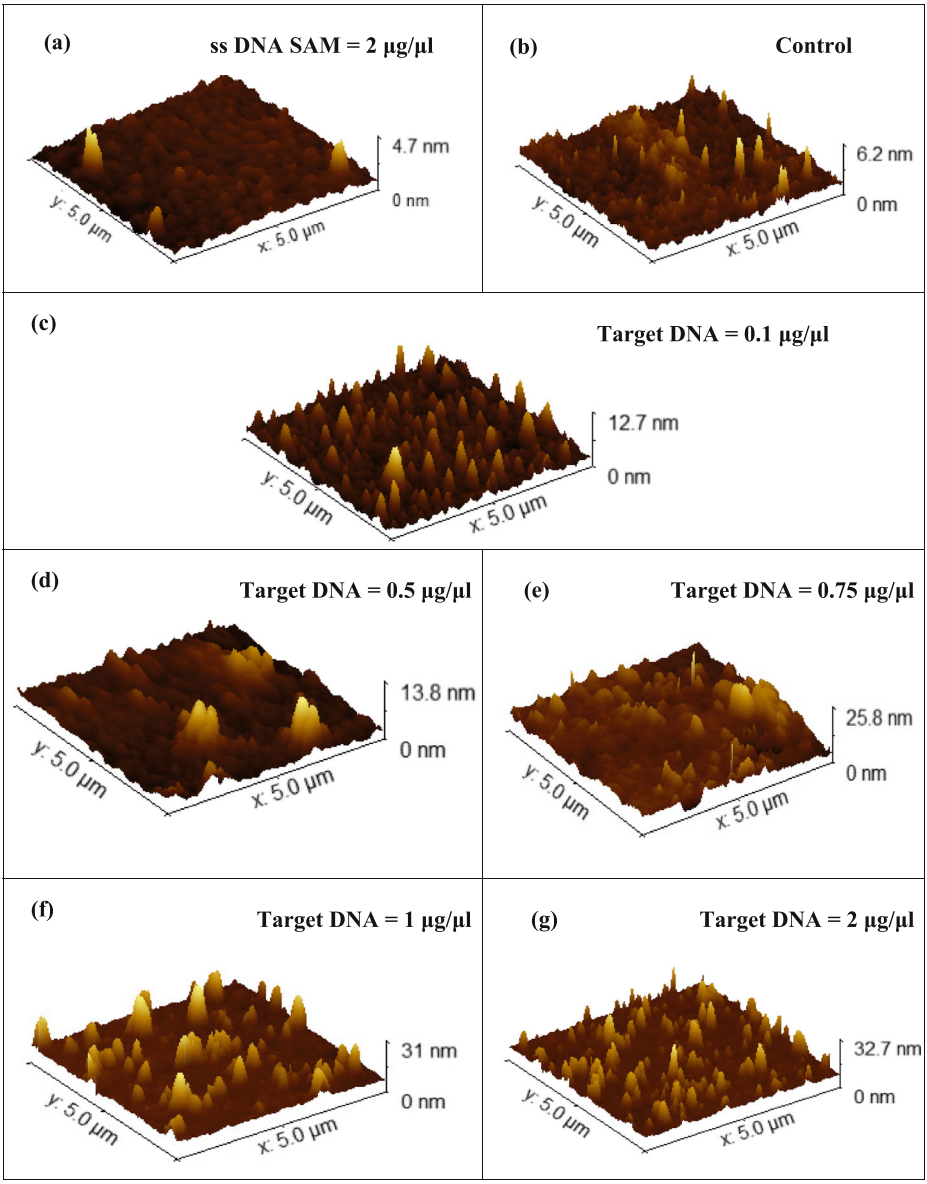

Fig. 8 Representative AFM images (5 × 5 µm) of different surface (**a**) ss DNA SAM (concentration = 2 µg/µl, time of incubation = 1 day); **b** the control experiment; **c**–**g** surface topography of different target DNA concentration ranging from 0.1 to 2 µg/µl

corresponding to a much lower level of adsorption. However, the adsorption of target DNA on top of the adsorbed layer resulted in much larger changes in the thickness. With the increase in the concentration from 0.1 to 2 µg/µl, the thickness of the surface increased from 12.5 ± 1.01 nm to 32 ± 2.15 nm, as can be seen in Fig. 8c–g. This showed that as the concentration increased, the agglomerated structure formation also increased.

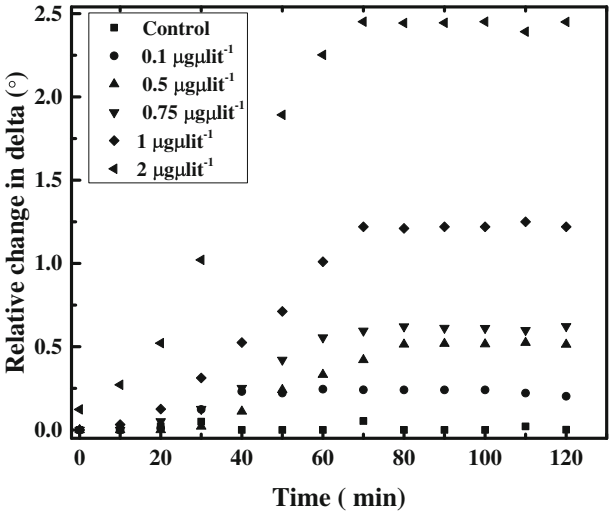

Fig. 9 Ellipsometric measurement of relative change in delta for control (■), 0.1 (●), 0.5 (▲), 0.75 (▼), 1 (♦), and 2 μg/μl (◀) target DNA concentration with variation in time

In order to evaluate the effect of incubation time, the hybridization measurements were monitored for 120 min and are shown in Fig. 9. To monitor the reaction, ellipsometry was performed on the surface every 10 min to obtain the ellipsometric parameters psi (Ψ) and delta (Δ). The optical properties are highly correlated with Δ (phase shift) and were monitored at different incubation times. During the hybridization process, with target DNA on the surface, the phase shift was altered based on the reflection of incident light [35]. From this change, the hybridization process can easily be monitored by ellipsometry. Firstly, a negative control experiment was performed with mismatched DNA at a concentration of 5 μg/μl in the same hybridization buffer to confirm the specificity of the captured DNA probe.

Figure 9 shows the relative change in delta-time curves for DNA hybridization on the modified surface. It can be seen that no significant change in delta–time curves was observed in the control experiments. This suggested that the addition of non-complementary DNA did not result in any shift in the delta spectra. Therefore, the effects of non-specific binding and non-specific hybridization were minimal. It can be seen that the target DNA hybridization depends on the concentration of target DNA.

Next, hybridization with specific target DNA was examined, which depends on the concentration of the various target DNA concentrations. In the control experiment, no significant change in Δ was observed. The data obtained showed that the hybridization process for different concentrations was completed at the very beginning of the hybridization (approximately 60 min) and then became saturated with a further increase in time. The relative changes in delta were 0.22° for 0.1 μg/μl, 0.51° for 0.5 μg/μl, 0.80° for 0.75 μg/μl, 1.22° for 1 μg/μl, and 2.45° for 2 μg/μl, respectively. After this time interval, the relative change in delta was almost constant, reaching a saturation value. This is consistent with results reported for biosensor preparation by use of gold nanoparticles [36]. This behavior may be due to a decreased driving force as a result of both the decrease in the DNA concentration in the

hybridization medium and decrement of available probes for interaction with time because of ongoing hybridization.

3.7 Reproducibility

The reproducibility of a DNA SAM biosensor was probed by repeating the measurements three times at a fixed concentration of *B. parapertussis* of 0.5 μg/μl. The reproducibility of ss DNA SAM was ± 0.3° with a relative change in Δ corresponding to 0.5 μg/μl of *B. parapertussis*. The surface-to-surface reproducibility of the ss DNA SAM biosensor was also determined between the surface synthesized and the variation coefficient was determined (3%), which was deemed a good number. To affirm the hybridization of *B. parapertussis* to ss DNA SAM, the ds DNA SAM was denatured to ss DNA SAM. Repeated AFM measurements were performed to confirm the ss DNA SAM surface reproducibility with a height variation of 6.42 ± 0.75 nm.

4 Conclusions

In this work, our aim was to use ss DNA SAM as a platform for the detection of *B. parapertussis* by ellipsometry. Selected ss DNA SAM were immobilized on the surface by disulfide bond formation. The results obtained by AFM and ellipsometry showed that prominent changes in thickness from 5.25 ± 0.84 to 14.40 ± 1.22 nm and in the refractive index from 1.489 to 1.652 were observed as the concentration of ss DNA SAM increased from 2 to 10 μg/μl for 1-day incubation. Finally, hybridization of target DNA with the immobilized ss DNA SAM was monitored by ellipsometry by measuring the relative change in delta (Δ) value. This showed that no prominent change in Δ was observed in the control experiment. In the case of complementary target DNA, the hybridization process completed rapidly and reached a saturation value in approximately 50 min for a 0.5 μg/μl concentration of target DNA. Therefore, we conclude that the present work is a quick (as it takes a few minutes for organization of a ss DNA SAM layer) and efficient approach to detect target DNA concentration of 0.1 μg/μl compared to PCR and DNA culture, which can be applied for the effective detection of *B. parapertussis*.

Acknowledgements This work was supported by the Higher Education Commission, Pakistan (HEC) development grant for 'Designing and Fabrication of Micro and Nano Devices' and the department of physics, COMSATS institute of Information Technology, Islamabad, Pakistan.

Compliance with ethical standards

Conflict of interest The authors declare that they have no conflicts of interest.

References

1. Templeton, K.E., Scheltinga, S.A., Van der Zee, A., Diederen, B.M.W., Kruijssen, A.M., Goossens, H., Kuijper, E., Claas, E.C.J.: Evaluation of real-time PCR for detection of and discrimination between *Bordetella pertussis*, *Bordetella parapertussis*, and *Bordetella holmesii* for clinical diagnosis. J. Clin. Microbiol. **41**, 4121–4126 (2003)

2. Bottero, D., Gaillard, M.E., Errea, A., Moreno, G., Zurita, E., Pianciola, L., Rumbo, M., Hozbor, D.: Outer membrane vesicles derived from *Bordetella parapertussis* as anacellular vaccine against *Bordetella parapertussis* and *Bordetella pertussis* infection. Vaccine. **31**, 5262–5268 (2013)
3. Bokhari, H., Said, F., Syed, M.A., Mughal, A., Kazi, Y.F., Heuvelman, K., Mooi, F.R.: Whooping cough in Pakistan: *Bordetella pertussis* vs *Bordetella parapertussis* in 2005-2009. Scand. J. Infect. Dis. **43**, 818–820 (2011)
4. Elahi, S., Thompson, D.R., Strom, S., O'Connor, B., Babiuk, L.A., Gerdts, V.: Infection with *Bordetella parapertussis* but not *Bordetella pertussis* causes pertussis-like disease in older pigs. J. Infect. Dis. **198**, 384–392 (2008)
5. Scanlon, K.M., Skerry, C., Carbonetti, N.H.: Novel therapies for the treatment of pertussis disease. Pathog. Dis. **73**, 1–9 (2015)
6. Cherry, J.D., Seaton, B.L.: Patterns of *Bordetella parapertussis* respiratory illnesses: 2008–2010. Clin. Inf. Dis. **54**, 534–537 (2012)
7. Mastrantonio, P., Stefanelli, P., Giuliano, M., Rojas, Y.H., Ciofi degli Atti, M., Anemona, A., Tozzi, A.E.: *Bordetella parapertussis* infection in children: epidemiology, clinical symptoms, and molecular characteristics of isolates. J. Clin. Microbiol. **36**, 999–1002 (1998)
8. Castillo, M.E., Bada, C., Aguila, D.O., Petrozzi-Helasvuo, V., Casabona-Ore, V., Reyes, I., Del Valle-Mendoza, J.: Detection of *Bordetella pertussis* using a PCR test in infants younger than one year old hospitalized with whooping cough in five Peruvian hospitals. Int. J. Inf. Dis. **41**, 36–41 (2015)
9. Nikbin, V.S., Shahcheraghi, F., Lotfi, M.N., Zahraei, S.M., Parzadeh, M.: Comparison of culture and real-time PCR for detection of *Bordetella pertussis* isolated from patients in Iran. Iran. J. Microbiol. **5**, 209–214 (2013)
10. Lind-Brandberg, L., Welinder-Olsson, C., Lagergård, T., Taranger, J,. Trollfors. B., Zackrisson, G.: Evaluation of PCR for diagnosis of *Bordetella pertussis* and *Bordetella parapertussis* infections. J. Clin. Microbiol. **36**, 679–683 (1998)
11. Kurbakov, K.A., Konorov, E.A., Minaev, M.Y., Kuznetsova, O.A. Multiplex real-time PCR assay for detection and differentiation of *Bordetella pertussis* and *Bordetella parapertussis*. Iran. J. Microbiol. **6**, 140–148 (2014)
12. Xu, Y., Xu, Y., Hou, Q., Yang, R., Zhang, S.: Triplex real-time PCR assay for detection and differentiation of *Bordetella pertussis* and *Bordetella parapertussis*. Acta Pathaologica Microbiologica et Immunologica Scandinavica. **118**, 685–691 (2010)
13. Md Eshrat, E.A., Subhas, C.M.: Detection methodologies for pathogen and toxins. Sensors **17**, 1885–1905 (2017)
14. Khalid, M.A., Mohammed, M.Z., Fouzi, M., Salman, A.A., Manal, A.A., Anees, A.A.: DNA-based nanobiosensors as an emerging platform for detection of disease. Sensors **15**, 14539–14568 (2015)
15. Razin, S.: DNA probes and PCR in diagnosis of mycoplasma infections. Mol. Cell. Probes **8**, 497–511 (1994)
16. Touahir, L., Allongue, P., Aureau, D., Boukherroub, R., Chazalviel, J.N., Galopin, E., Gouget-Laemmel, A.C., de Villeneuve, C.H., Moraillon, A., Niedziółka-Jönsson, J., Ozanam, F., Andresa, J.S., Sam, S., Solomon, I., Szunerits, S.: Molecular monolayers on silicon as substrates for biosensors. Bioelectrochem. **80**, 17–25 (2010)
17. Georgiadis, R., Peterlinz, K.P., Peterson, A.W.: Quantitative measurements and modeling of kinetics in nucleic acid monolayer films using SPR spectroscopy. J. Am. Chem. Soc. **122**, 3166–3173 (2000)
18. Kewu, L., Shuang, W., Liming, W., Hui, Y., Ning, J., Rui, X., Zhibin, W.: Fast and sensitive ellipsometry-based biosensing. Sensors **18**, 1–13 (2018)
19. Javed, S., Said, F., Bokhari, H.: *Bordetella parapertussis* outbreak in Bisham, Pakistan in 2009-2010: fallout of the 9/11 syndrome. Epidemiol. Infect. **143**, 2619–2623 (2015)
20. Xing, W., Cheng, J.: Electronic biosensor based on DNA self-assembled monolayer on gold electrode, Frontiers in Biochip Technology, Springer (2005).
21. Herne, T.M., Tarlov, M.J.: Characterization of DNA probes immobilized on gold surfaces. J. Am. Chem. Soc. **119**, 8916–8920 (1997)
22. Bokhari, H., Said, F., Syed, M.A., Hussain, A., Kazi, Y.F., Kallonen, T., He, Q., King, A.J., Heuvelman, K., Mooi, F.R.: Molecular typing of *Bordetella parapertussis* isolates circulating in Pakistan. FEMS Immunol. Med. Microbiol. **63**, 373–380 (2011)
23. Kriechbaumer, V., Tsargorodskaya, A., Mustafa, M.K., Vinogradova, T., Lacey, J., Smith, D.P., Abell, B.M., Nabok, A.: Study of receptor-chaperone interactions using the optical technique of spectroscopic ellipsometry. Biophys. J. **101**, 504–511 (2011)
24. Ieva, B., Zigmas, B., Asta, M., Almira, R., Arunas, R.: Study of antibody/antigen binding kinetics by total internal reflection ellipsometry. Biosens. Bioelectron. **39**, 170–176 (2013)

25. Campos-Ferreira, D.S., Souza, E.V.M., Nascimento, G.A., Zanforlin, D.M.L., Arruda, M.S., Beltrao, M.F., Melo, S.A.L., Bruneska, D., Lima-Filho, J.L.: Electrochemical DNA biosensor for the detection of human papillomavirus E6 gene inserted in recombinant plasmid. Arab. J. Chem. **9**, 443–450 (2016)
26. Miriam, C., Florent, P., Olivier, M., Judikael, L.R., Gerard, B., Rose-Marie, S., Jorg, A., Ludocic, E.: Spectroscopic ellipsometry study of silver nanospheres and nanocubes in thin film layers. Opt. Mater. Express **7**, 4241–4249 (2017)
27. Nabok, A.V., Tsargorodskaya, A., Holloway, A., Starodub, N.F., Gojster, O.: Registration of T-2 mycotoxin with total internal reflection ellipsometry and QCM impedance methods. Biosens. Bioelectron. **22**, 885–890 (2007)
28. Tikhonravov, A.V., Trubetskov, M.K., Masetti, E., Krasilnikova, A.V., Kochikov, I.V.: Sensitivity of the ellipsometric angles psi and delta to the surface inhomogeneity. Conf Adv Opt Interference Coatings **3738**, 0277–786X (1999)
29. Nabok, A., Tsargorodskayaa, A., Mustafa, M.K., Szekacs, I., Starodub, N.F., Szekacs, A.: Detection of low molecular weight toxins using an optical phase method of ellipsometry. Sensors Actuators B Chem. **154**, 232–237 (2011)
30. Legay, G., Markey, L., Meunier- Prest, R., Finot, E.: Measurements of thickness dispersion in biolayers by scanning force microscopy and comparison with spectroscopic ellipsometry analysis. Ultramicroscopy **107**, 1111–1117 (2007)
31. Hwall, M., Eugene, F., Weiwei, Z., Chowdhury, A., David, A., Adri, C.T.D., Srinivas, T.: Modified random sequential adsorption model for understanding kinetics of proteins adsorption at a liquid–solid interface. Langmuir **33**, 7215–7224 (2017)
32. Corsel, J.W., Williems, G.M., Kop, J.M., Cuypers, P.A., Hermensn, W.T.: The role of intrinsic binding rate and transport rate in the adsorption of prothrombin, albumin, and fibrinogen to phospholipid bilayers. J. Colloid Interface Sci. **111**, 544–554 (1986)
33. Pearson, C.E., Wang, Y., Griffith, J.D., Sinden, R.R.: Structural analysis of slipped-strand DNA (S-DNA) formed in (CTG)n. (CAG)n repeats from the myotonic dystrophy locus. Nucleic Acids Res. **26**, 816–882 (1998)
34. Sun, Y., Zhu, X.: An ellipsometry-based biosensor for label-free, real-time, and in-situ detection of DNA–DNA and DNA–protein interactions. Chinese J. Phy. **52**, 1398–1406 (2014)
35. Demirel, G., Mustafa, O.C., Garipcan, B., Piskin, E.: A novel DNA biosensor based on ellipsometry. Surf. Sci. **602**, 952–959 (2008)
36. Mustafa, O.Ç., Filiz, S., Gökhan, D., Bora, G., Burcu, O., Burcu, Ç., Erhan, P.: Stepwise formation approach to improve ellipsometric biosensor response. Nanomedicine **5**, 152–161 (2009)

Affiliations

S. Rafique[1] · M. Idrees[2] · H. Bokhari[2] · A. S. Bhatti[3]

[1] Department of Physics, Air University, PAF Complex, E-9, Islamabad 44000, Pakistan

[2] Department of Microbiology, COMSATS Institute of Information Technology, Islamabad 44000, Pakistan

[3] Centre for Micro & Nano Devices, Department of Physics, Faculty of Science, COMSATS Institute of Information Technology, Park Road Campus, Islamabad 44000, Pakistan